

## Ultrafast carrier dynamics in CuInS<sub>2</sub> quantum dots

Jianhui Sun, Dehua Zhu, Jialong Zhao, Michio Ikezawa, Xiuying Wang, and Yasuaki Masumoto

Citation: *Applied Physics Letters* **104**, 023118 (2014); doi: 10.1063/1.4862274

View online: <http://dx.doi.org/10.1063/1.4862274>

View Table of Contents: <http://scitation.aip.org/content/aip/journal/apl/104/2?ver=pdfcov>

Published by the [AIP Publishing](#)

---

### Articles you may be interested in

[Multilevel characteristics and memory mechanisms for nonvolatile memory devices based on CuInS<sub>2</sub> quantum dot-polymethylmethacrylate nanocomposites](#)

*Appl. Phys. Lett.* **105**, 233303 (2014); 10.1063/1.4903243

[Evidence of significant down-conversion in a Si-based solar cell using CuInS<sub>2</sub>/ZnS core shell quantum dots](#)

*Appl. Phys. Lett.* **104**, 183902 (2014); 10.1063/1.4875616

[Shell-thickness-dependent photoinduced electron transfer from CuInS<sub>2</sub>/ZnS quantum dots to TiO<sub>2</sub> films](#)

*Appl. Phys. Lett.* **102**, 053119 (2013); 10.1063/1.4790603

[An energy-harvesting scheme utilizing Ga-rich CuIn\(1-x\)GaxSe<sub>2</sub> quantum dots for dye-sensitized solar cells](#)

*Appl. Phys. Lett.* **101**, 123901 (2012); 10.1063/1.4751469

[Electrical characteristics and operating mechanisms of nonvolatile memory devices fabricated utilizing core-shell CuInS<sub>2</sub>-ZnS quantum dots embedded in a poly\(methyl methacrylate\) layer](#)

*Appl. Phys. Lett.* **99**, 193302 (2011); 10.1063/1.3659473

---

The advertisement features a photograph of the Model PS-100 cryogenic probe station, which is a complex piece of scientific equipment with various mechanical components and a probe. The background is a gradient of blue. The text is arranged around the image: the model name and description on the left, the company logo on the right, and a slogan at the bottom right.

**Model PS-100**  
Tabletop Cryogenic  
Probe Station

The logo for Lake Shore CRYOTRONICS consists of a stylized blue and white square icon to the left of the company name. 'Lake Shore' is in a large, white, serif font, and 'CRYOTRONICS' is in a smaller, white, sans-serif font below it.

*An affordable solution for  
a wide range of research*

## Ultrafast carrier dynamics in CuInS<sub>2</sub> quantum dots

Jianhui Sun,<sup>1,2,3</sup> Dehua Zhu,<sup>4</sup> Jialong Zhao,<sup>2,4,a)</sup> Michio Ikezawa,<sup>1</sup> Xiuying Wang,<sup>2</sup> and Yasuaki Masumoto<sup>1,b)</sup>

<sup>1</sup>*Institute of Physics, University of Tsukuba, Tsukuba 305-8571, Japan*

<sup>2</sup>*State Key Laboratory of Luminescence and Applications, Changchun Institute of Optics, Fine Mechanics and Physics, Chinese Academy of Sciences, Changchun 130033, China*

<sup>3</sup>*University of Chinese Academy of Sciences, Beijing 100039, China*

<sup>4</sup>*College of Mechanical and Electrical Engineering, Wenzhou University, Wenzhou 325035, China*

(Received 5 November 2013; accepted 29 December 2013; published online 16 January 2014)

The ultrafast carrier dynamics in CuInS<sub>2</sub> (CIS) quantum dots (QDs) was studied by means of femtosecond transient absorption (TA) spectroscopy. The size-dependent 1S transition energy determined from bleaching spectra is in agreement with that calculated on the finite-depth-well model in the effective mass approximation. The TA bleaching comes from filling of electron quantized levels, allowing us to know the dynamics of the 1S electron in CIS QDs. The sub-100-ps electron trapping at surface defects in bare QDs accelerates with decreasing QD size, while is effectively suppressed in well-passivated CIS/ZnS core/shell QDs. © 2014 AIP Publishing LLC. [<http://dx.doi.org/10.1063/1.4862274>]

Quantum dots (QDs) exhibit profound size-dependent optical and electronic properties, having attracted much interests in both fundamental science and applications to solar cells<sup>1,2</sup> and light emitting diodes.<sup>3,4</sup> The carrier relaxation in QDs is extremely sensitive to the surface characteristics due to the considerable surface-to-volume ratio. The defects on the QD surface, such as the dangling bonds, act as the trap states near the band edge. In most cases, carrier trapping at the surface defects takes place in less than 100 ps in CdS<sup>5</sup> and CdSe<sup>6–9</sup> QDs. The fast carrier-trapping significantly reduces the efficiency of the band-edge photoluminescence (PL). As alternatives to II–VI QDs, chalcopyrite-type I–III–VI<sub>2</sub> QDs have been proposed because of their less-toxic components. Among them, CuInS<sub>2</sub> (CIS) QDs are important candidates for optoelectronic devices, because bulk CIS has a direct band gap of 1.53 eV.<sup>10–13</sup> Naturally, the ultrafast carrier dynamics in CIS QDs have become of great interest.

Recently, it has been demonstrated that the radiative recombination in CIS QDs involves a transition associated with the localized intragap state,<sup>10,12</sup> since it showed the long emission-lifetimes as well as the large Stokes-shift between the PL band and the band-edge absorption in CIS QDs. However, the band-edge-carrier localization by intragap states in CIS QDs is ambiguous, leading to be unable to clarify the origin of the PL in CIS QDs. It is because the radiative recombination in CIS QDs does not come from the band-edge transitions. The dynamics of the band-edge carriers cannot be directly resolved in the time-resolved PL spectroscopy.<sup>11,12</sup> In contrast, the transient absorption (TA) spectra are dominated by filling of the lowest 1S quantized levels and the dynamics of the band-edge carriers such as the 1S electron trapping at the surface defects can be well resolved.

Here, we investigated the mechanisms for optical nonlinearities and ultrafast carrier dynamics in CIS QDs by means of femtosecond TA spectroscopy. We observed a nearly

symmetrical bleaching band and a broad photoinduced absorption (PA) region in the TA spectra. Furthermore, we measured the laser-intensity dependence of the TA to confirm that the band-edge bleach in CIS QDs is dominated by filling of 1S electron states. From the initial decay of the bleaching, the surface trapping of the 1S electrons had been studied in CIS core and CIS/ZnS core/shell QDs.

We synthesized the CIS core and CIS/ZnS core/shell QDs by a typical wet chemical method.<sup>10</sup> The average diameters of three kinds of CIS core QDs were determined to be 2.5, 3.3, and 4.0 nm, respectively, by means of transmission electron microscopy. The white-light femtosecond TA spectrometer used in this study is based on a regeneratively amplified Ti:sapphire laser system (Spectra-Physics, 800 nm, 130 fs, and 1 kHz repetition rate). Pump pulses at 400 nm were generated by frequency doubling of the 800 nm laser beam in a  $\beta$ -barium borate (BBO) crystal 2 mm thick. The white-light probe was generated by focusing the 800 nm laser beam onto a sapphire plate 2 mm thick. The QDs dispersed in toluene were sealed in quartz cells 1 mm thick for all the TA measurements. During the data collection, samples were constantly moved in X–Y directions at a speed of 10 cm/min to avoid the degradation of the samples. We confirmed that there was no detectable change of the samples in both the absorption spectra and the absorption peak values between before and after the measurements.

The steady-state absorption, PL, and TA spectra for CIS QDs grown at 230 °C are shown in Fig. 1(a). The absorption edge and PL band gradually shift toward longer wavelength with increasing diameter of the QDs, in consistent with quantum confinement effect. Like the previous reports,<sup>10–12</sup> no sharp excitonic absorption peak was observed in the steady-state absorption spectra. It is well known that the presence of discrete electronic states is masked in the linear absorption spectra by large inhomogeneous broadening in CIS QDs.<sup>12,14</sup> Each QD may vary in size, geometry, and stoichiometry, especially for CIS QDs because of their ternary chemical-composition. These variations cause a strong inhomogeneous broadening of the optical transitions. In contrast, the structures

<sup>a)</sup>Electronic mail: zhaojl@ciomp.ac.cn

<sup>b)</sup>Electronic mail: masumoto@physics.px.tsukuba.ac.jp. URL: <http://www.sakura.tsukuba.ac.jp/~ikezawa/lab/>.

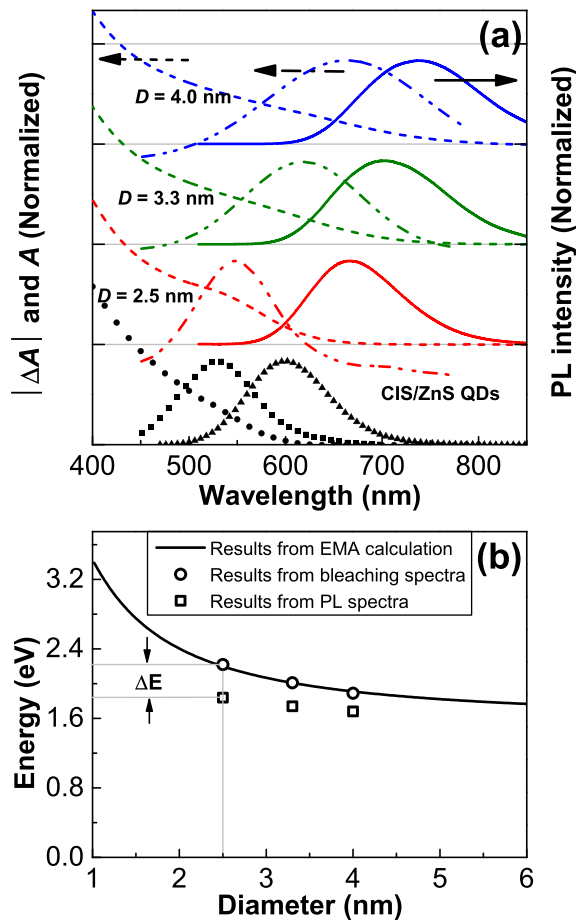


FIG. 1. (a) Steady-state absorption ( $A$ ) (dashed lines), PL spectra (solid lines) and TA spectra (dashed dotted lines) of CIS QDs with three average diameters. Steady-state absorption (circles), PL spectra (triangles), and TA spectra (squares) of CIS/ZnS core/shell QDs with core diameters of 2.5 nm.  $\Delta A$  and PL normalized by their peak values.  $A$  normalized at 450 nm. For TA measurement, the pump fluence is set to  $\langle N_0 \rangle = 0.5$  for each sample (average number of absorbed photons equals to 0.5) at wavelength of 400 nm and pump-probe delay time is 4 ps; (b) the size-dependent 1S transitions determined from bleaching spectra is illustrated by circles and size-dependent energy levels of PL are illustrated by squares. The solid line represents the calculated band gaps as a function of the diameters of CIS QDs on the finite-depth-well model in the EMA.

of the 1S transition can be well resolved in nonlinear TA spectra, as shown by dotted lines in Fig. 1(a). This is because the nonlinear TA spectra are dominated by bleaching the 1S transitions after the fast intraband carrier relaxation is completed.

Furthermore, we calculated the band gaps of CIS QDs on the finite-depth-well model in the effective mass approximation (EMA). The effective masses of electrons and holes are  $0.16 m_0$  and  $1.30 m_0$ , respectively, where the  $m_0$  is the electron mass in vacuum.<sup>12</sup> As shown in Fig. 1(b), size-dependent 1S transition energy determined from bleaching spectra is in agreement with that calculated. On the other hand, the emission peak deviates from its corresponding band gap calculated, and the deviation, that is Stokes shift, increases up to 0.38 eV with the decrease in the size of CIS QDs. Besides, it was reported that the radiative recombination in CIS QDs showed the long emission-lifetime of more than 300 ns.<sup>10,19</sup> This suggests that the radiative recombination does not come from band-edge transition.

We investigated the laser-intensity dependence of the TA to understand the intrinsic characters of the carrier in

CIS QDs. Two features are observed in the TA spectra presented in Fig. 2(a): a rather symmetrical bleaching band and a broad PA region extending to low-energy side in the spectra. The bleaching of 1S transitions increases with the increase of pump fluence. As shown in Fig. 2(b), the bleaching saturated at higher fluence indicates that the degeneracy of 1S transitions is finite in CIS QDs. It had been suggested that the band-edge bleach at room temperature is dominated by filling of 1S electron states without a discernible contribution from holes in CIS QDs.<sup>10</sup> This is because the degeneracy of the valence band is much larger than that of the conduction band, which is a combined result of the large difference between electron and hole masses ( $m_h/m_e = 8$ ) and the multiband structure of the valence band in CIS.

When the pump-photon energy (3.1 eV) is much higher than the band gap of QDs so that the saturation at the pump wavelength is insignificant, the populations in the QDs following the Poisson distribution:  $P(N) = \langle N \rangle^N e^{-\langle N \rangle} / N!$  can be calculated, where  $P(N)$  is the probability of having  $N$  electron-hole pairs in a dot in case the average populations of QDs are  $\langle N \rangle$ .<sup>8,15</sup> The 1S absorption change ( $\Delta A$ ) is proportional to the population of the 1S electron state. It can be expressed as  $\Delta A \propto \langle n_{1S} \rangle$ , where  $\langle n_{1S} \rangle$  is the average occupation number of the 1S electron state. Because of the twofold spin degeneracy for the 1S electron state (shown in the inset in Fig. 2(b)),  $\langle n_{1S} \rangle$  can be calculated as:  $\langle n_{1S} \rangle = 1 - e^{-\langle N \rangle} (1 + \langle N \rangle / 2)$ .<sup>15</sup> At the initial stage ( $\Delta t = 4$  ps) of the 1S electron relaxation,  $\langle N \rangle$  is directly proportional to the pump fluence ( $j_p$ ) and can be expressed as:  $\langle N \rangle = j_p \sigma_a$ ,<sup>16</sup> in which the  $\sigma_a$  is the absorption

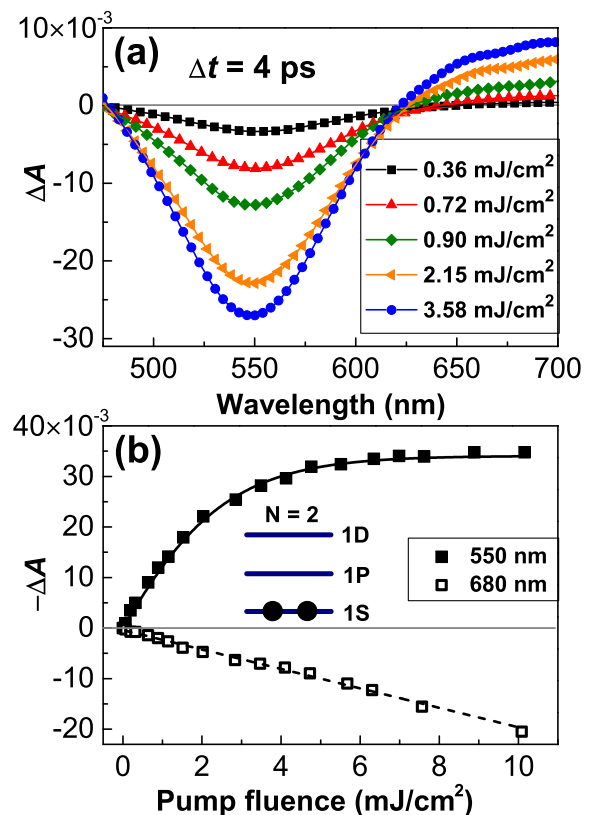


FIG. 2. (a) TA spectra of CIS QDs 2.5 nm in diameter recorded at five pump fluences. (b) The bleach amplitude of CIS QDs at the 1S absorption peak as a function of the pump fluence. Pump-probe delay time is 4 ps and the solid line is the best fit by Eq. (1) in the text.

cross section of a QD at the excitation wavelength of 400 nm.<sup>17</sup> Therefore, we obtain the following expression:<sup>8,15,17</sup>

$$\langle n_{1S} \rangle = 1 - e^{-j_p \sigma_a} (1 + j_p \sigma_a / 2). \quad (1)$$

The pump-fluence-dependent changes of the 1S absorption can be well fitted by Eq. (1). As seen in Fig. 2(b), the data show the initial linear growth followed by saturation similarly to the behavior observed in CdSe QDs.<sup>8,15</sup> The fitting yields  $\sigma_a$  of  $3.9 \times 10^{-16}$  (cm<sup>2</sup>), which is comparable to the calculated value of  $3.5 \times 10^{-16}$  (cm<sup>2</sup>) for a 2.5 nm CIS QD at the wavelength of 400 nm.<sup>10</sup> The good fit confirms that the band-edge bleach in CIS QDs is dominated by filling of 1S electron states.

The PA observed in QDs is associated with either the Coulomb multiparticle interactions, such as the biexciton effect<sup>8,14</sup> or the trapped-carrier related excited-state absorption.<sup>15</sup> Although the ground biexciton states can be formed in CIS QDs, the sharp biexcitonic features are not observed probably due to the broadening of the 1S bleach band. As shown in Fig. 2(a), there is no wavelength selectivity in the spectra of PA of CIS QDs. Moreover, the PA signals show the linear growth with the pump fluence and do not show saturation as shown by hollow squares in Fig. 2(b). Therefore, the spectrally broad PA observed in CIS QDs most likely originates from the transition of carriers trapped at defect states. Furthermore, the PA observed in well-passivated CIS/ZnS core/shell QDs indicated that carriers are trapped even inside the CIS QDs, consistent with the recent report claiming the internal defect states stem from the substitution of the copper and indium ions in CIS QDs.<sup>10</sup>

It is an important concern that a high probability of the carrier trapping at surface defects degenerates the performance of QD-based optoelectronic devices.<sup>10,18,19</sup> In our previous work,<sup>19</sup> we found that the low efficiency of the electron injection into TiO<sub>2</sub> films from small CIS QDs was attributed to the large amount of surface-localized states. Recently, the carrier trapping in CIS QDs has been studied mainly by means of time-resolved PL spectroscopy.<sup>10-13</sup> These reports show that the luminescence of the CIS QDs is significantly reduced due to the surface trapping effects. However, it is unable to distinguish the electron and hole trapping at the trap states in the time-resolved PL spectroscopy, because both electrons and holes contribute to the PL dynamics.<sup>8</sup> As discussed above, the TA spectra are dominated by filling of 1S electron states after the intraband relaxation. Therefore, we can use the 1S bleaching decay dynamics to evaluate the depopulation rate of the 1S electrons in CIS QDs. The 1S electron relaxation paths in CIS QDs can be clearly revealed.

For all the decay curves shown in Fig. 3, the TA kinetics cannot be fitted by a single-exponential decay. The TA kinetics show two distinct regions: the initial fast decay in sub-100-ps followed by slow nanosecond decay. A quantitative analysis of the decay curves was carried out by a simple bi-exponential fit. The initial decay in sub-100-ps as well as the corresponding signal decrease is sensitive to the size of the CIS QDs. In smallest CIS QDs, the population of 1S electron decreases quickly at a time constant of 14 ps by 23% of the initial peak amplitude followed by a slow 1.8 ns decrease by 77% of the initial peak amplitude. The TA measurement

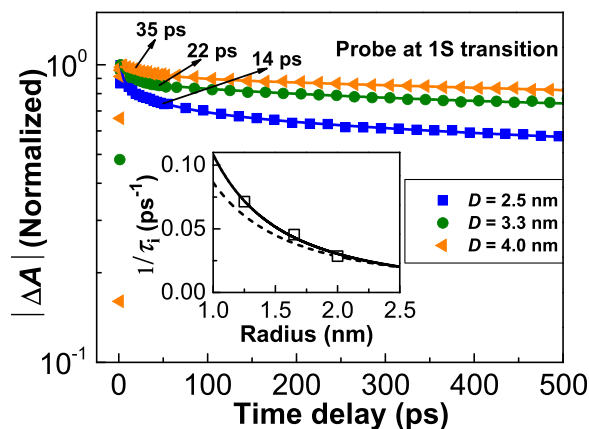


FIG. 3. The normalized TA kinetics of CIS QDs with three diameters. The rates of the electron trapping are plotted in the inset by hollow squares. The solid line in the inset shows the fit by a power-law expression. The calculated electron densities at the QD surface as a function of radius are shown by dashed line in the inset. The electron densities were normalized to the slowest measured-trapping-rate for comparison.

was performed in the low-intensity excitation regime (average number of absorbed photons equals to 0.5) where the fast multiparticle Auger recombination was insignificant.<sup>7,8</sup> The initial 14 ps decay is most likely due to the electron relaxation from the 1S state to a new state, such as the surface-defect state in the band gap. The inset in Fig. 3 shows a plot of initial-decay rate ( $1/\tau_i$ ) for the average radius ( $R$ ). The initial-decay rates slow markedly as the QD radius increases. The solid line in the inset in Fig. 3 shows the best fit of these data by a power-law expression:  $1/\tau_i = CR^n$ , where  $C$  is a constant and  $n$  describes the order. The fitting yields  $n$  of  $-1.8$ , which is comparable to the reported one ( $-1.5$ ) for CdSe QDs.<sup>20</sup> The electron capture rate at the surface of CIS QDs was evaluated to explain the relationship between QDs radius and the initial-decay rate. The details of the calculation were described previously.<sup>19</sup> As shown in the inset in Fig. 3, the calculated radial electron densities at the QD surface as a function of QD radius follow the size dependence of  $R^{-1.6}$ , in reasonable agreement with the size dependence of the initial-decay rate of  $R^{-1.8}$ . The agreement with the calculation indicates that the initial-decay rate is proportional to the existing probability of electron at the QD surface. Therefore, the initial decay in sub-100-ps in CIS QDs is due to the electron relaxation from the 1S state to the surface-defect state.

We further investigated the 1S electron trapping at the defects by making ZnS shells on 2.5 nm CIS core QDs. After overcoating with ZnS, the quantum yield of PL increased from 3.5% in the core QDs to 81% in the CIS/ZnS core/shell QDs. The significant increase in efficiency of the band-edge PL indicates that the surface defects in bare QDs are effectively passivated by ZnS shells. As seen in Fig. 4, the bleaching in CIS/ZnS core/shell QDs recovers extremely slowly in contrast with the fast recovery of the bleaching in CIS core QDs. The initial-decay time increased up to 91 ps with a small decay amplitude of 1.3%. The improvement in surface passivation leads to the suppression of the fast decay component, confirming that the fast decay component comes from electrons trapping at surface defects. However, the PA is observed at the lower energy side of the bleaching band in well-passivated CIS/ZnS core/shell QDs, as shown in

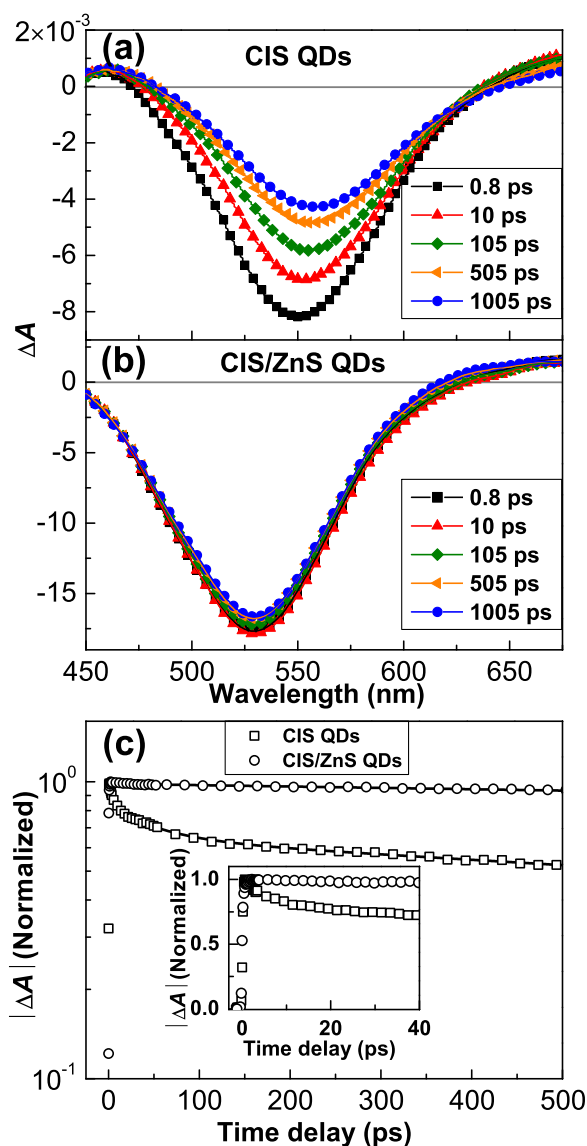


FIG. 4. TA spectra of (a) CIS QDs 2.5 nm in diameter and (b) CIS/ZnS core/shell QDs with core diameters of 2.5 nm. (c) The normalized TA kinetics of CIS QDs and CIS/ZnS core/shell QDs. The inset shows the enlarged TA kinetics in a short time scale. The probe wavelength for CIS and CIS/ZnS core/shell QDs is 550 and 530 nm, respectively.

Fig. 4(b). The observed PA in CIS/ZnS core/shell QDs comes from electrons trapped at the higher-energy states associated with internal defects. Besides, the 1S bleaching spectra show the red shift (about 10 nm) as the time proceeds in CIS core QDs. This indicates that the different relaxation behavior is associated with a size inhomogeneity in CIS core QDs. The relaxation of the 1S electrons is faster in smaller QDs with larger density of electrons at surface.

The PL in CIS QDs had been previously attributed to the recombination of donor-acceptor pairs.<sup>13</sup> In recombination of donor-acceptor pairs, the electrons and holes at the band edge are fast trapped by the donors (about 10–20 ps) and the acceptors (within 1 ps), respectively, and then the trapped electron-hole pairs recombine to emit photons.<sup>5</sup> However, high quantum yield of PL in CIS/ZnS QDs with little fast electron-localization contradicts the previous report. The localized carrier in CIS QDs must be the hole and the long-

lifetime emission is most entirely involved with the transition from a 1S electron state to a hole-localized state.

In summary, we have investigated the mechanisms for optical nonlinearities and ultrafast carrier dynamics in CIS QDs by means of femtosecond TA spectroscopy. The size-dependent 1S transition energy was obtained from bleaching spectra in agreement with the calculated one. From pump-intensity dependence of the TA spectra, we found that the 1S absorption changes as a function of pump fluence could be well fitted on the state-filling model assuming the Poisson distribution of electron populations. Therefore, the TA bleaching in CIS QDs is dominated by filling of the 1S electron states. Based on such a verdict, the ultrafast electron dynamics was investigated in CIS QDs. The decay in sub-100-ps is due to the electron relaxation from the 1S state to a surface-defect state. We found that the sub-100-ps electron trapping in bare QDs accelerated with decreasing QDs size. The rates of the electron trapping were shown to scale with the inverse of QD radius ( $1/\tau_1 \propto R^{-1.8}$ ). These surface trapping states were effectively passivated in CIS/ZnS core/shell QDs. The experimental results clearly show the intrinsic characters of the 1S electron states in CIS QDs and the way to further optimize the CIS QDs-based optoelectronic devices.

This work was supported by Grant-in-Aid for the Scientific Research from the MEXT of Japan (No. 23340084) and the National Natural Science Foundation of China (Nos. 11274304 and 51102227).

- <sup>1</sup>W. U. Huynh, J. J. Dittmer, and A. P. Alivisatos, *Science* **295**, 2425 (2002).
- <sup>2</sup>I. Gur, N. A. Fromer, M. L. Geier, and A. P. Alivisatos, *Science* **310**, 462 (2005).
- <sup>3</sup>S. Coe, W. K. Woo, M. Bawendi, and V. Bulović, *Nature* **420**, 800 (2002).
- <sup>4</sup>J. L. Zhao, J. A. Bardecker, A. M. Munro, M. S. Liu, Y. H. Niu, I. K. Ding, J. D. Luo, B. Q. Chen, A. K.-Y. Jen, and D. S. Ginger, *Nano Lett.* **6**, 463 (2006).
- <sup>5</sup>V. I. Klimov, P. H. Bolivar, and H. Kurz, *Phys. Rev. B* **53**, 1463 (1996).
- <sup>6</sup>V. I. Klimov and D. W. McBranch, *Phys. Rev. Lett.* **80**, 4028 (1998).
- <sup>7</sup>V. I. Klimov, A. A. Mikhailovsky, D. W. McBranch, C. A. Leatherdale, and M. G. Bawendi, *Science* **287**, 1011 (2000).
- <sup>8</sup>V. I. Klimov, *J. Phys. Chem. B* **104**, 6112 (2000).
- <sup>9</sup>P. T. Jing, W. Y. Ji, X. Yuan, M. Ikezawa, L. G. Zhang, H. B. Li, J. L. Zhao, and Y. Masumoto, *J. Phys. Chem. Lett.* **4**, 2919 (2013).
- <sup>10</sup>L. Li, A. Pandey, D. J. Werder, B. P. Khanal, J. M. Pietryga, and V. I. Klimov, *J. Am. Chem. Soc.* **133**, 1176 (2011).
- <sup>11</sup>X. Yuan, J. L. Zhao, P. T. Jing, W. Zhang, H. B. Li, L. G. Zhang, X. H. Zhong, and Y. Masumoto, *J. Phys. Chem. C* **116**, 11973 (2012).
- <sup>12</sup>H. Zhong, S. S. Lo, T. Mirkovic, Y. Li, Y. Ding, Y. Li, and G. D. Scholes, *ACS Nano* **4**, 5253 (2010).
- <sup>13</sup>B. Chen, H. Zhong, W. Zhang, Z. Tan, Y. Li, C. Yu, T. Zhai, Y. Bando, S. Yang, and B. Zou, *Adv. Funct. Mater.* **22**, 2081 (2012).
- <sup>14</sup>V. I. Klimov, S. Hunsche, and H. Kurz, *Phys. Rev. B* **50**, 8110 (1994).
- <sup>15</sup>*Semiconductor and Metal Nanocrystals: Synthesis and Electronic and Optical Properties*, edited by V. I. Klimov (Dekker, New York, 2004).
- <sup>16</sup>The pump fluence ( $J_p$ ) is presented in terms of the number of photons per  $\text{cm}^2$ .
- <sup>17</sup>J. Nanda, S. A. Ivanov, H. Htoon, I. Bezel, A. Piryatinski, S. Tretiak, and V. I. Klimov, *J. Appl. Phys.* **99**, 034309 (2006).
- <sup>18</sup>K. Dohnalová, A. N. Poddubny, A. A. Prokofiev, W. D. de Boer, C. P. Umesh, J. M. Paulusse, H. Zuillhof, and T. Gregorkiewicz, *Light: Sci. Appl.* **2**, e47 (2013).
- <sup>19</sup>J. H. Sun, J. L. Zhao, and Y. Masumoto, *Appl. Phys. Lett.* **102**, 053119 (2013).
- <sup>20</sup>S. L. Sewall, R. R. Cooney, K. E. H. Anderson, E. A. Dias, D. M. Sagar, and P. Kambhampati, *J. Chem. Phys.* **129**, 084701 (2008).